Eur Biophys J (1987) 15: 159–168

European Biophysics Journal

Kinetic study of the self-assembly of brome mosaic virus capsid

C. Berthet-Colominas [1] *, M. Cuillel [1], M. H. J. Koch [2], P. Vachette [3], and B. Jacrot [1]

[1] EMBL Outstation c/o ILL, F-38042 Grenoble-Cedex, France
[2] EMBL Outstation c/o DESY, Notkestrasse 85, D-2000 Hamburg 52, Federal Republic of Germany
[3] LURE, Université Paris Sud, F-91405 Orsay, France

Received December 5, 1986/Accepted in revised form April 30, 1987

Abstract. The protein of brome mosaic virus can self assemble in-vitro to form empty capsids. In the absence of RNA at pH = 7 and 0.5 *M* KCl there is a dynamic equilibrium between monomers and oligomers. At pH = 5 the protein assembles into empty capsids. The kinetics of this assembly, triggered by pH jump from neutral to acidic pH, was investigated by X-ray and light scattering.

Cryoelectron microscopy observations suggested that reconstitution is achieved by progressive incorporation of small building units in a spherical shell. This hypothesis has been tested by the analysis of the scattering data in terms of four classes of incomplete capsids represented as spherical shells with holes of different sizes. The time dependence of the population of each class was determined by a least squares analysis of the experimental data. Although the basic polymerizing unit has not been uniquely characterized, the results are compatible with a dimer for this species. The characteristic times for capsid assembly are found to vary as the inverse of the square of the concentration.

Key words: Plant virus, morphogenesis, kinetic, X-rays, light scattering

Introduction

Virus morphogenesis is an important step in the infection cycle of many viruses. In vitro assembly, which may follow a different pathway than in vivo, can give information about the built-in recognition mechanisms between viral components. In this respect, brome mosaic virus is a particularly interesting system which allows one to study both the assembly of the virus and of the capsid.

Brome mosaic virus (BMV) is a small plant virus of 13.4 nm radius which possesses a divided genome of single stranded RNA contained in a protein capsid composed of 180 copies of a single polypeptide. The molecular weight of the virus is 4.6×10^6 dalton. The proteins are located at quasi-equivalent sites on an icosahedron of triangulation number $T = 3$. Electron microscopy observations on the related cowpea chlorotic mottle virus (CCMV) using negative staining, indicate that the proteins are clustered in 12 pentamers and 20 hexamers (Steven et al. 1978).

BMV constitutes a simple model (Kaper 1975) of a virus with protein-protein interactions strong enough to allow the formation (in vitro but not in vivo) of empty capsids in the absence of RNA. These interactions are dependant on the physical conditions (pH, temperature, pressure) and consequently, there are at least two states of aggregation of the protein: dimers and capsids (Pfeiffer and Hirth 1974). Beside the protein-protein interactions, the protein-nucleic acid interactions determine the overall stability of the virus.

Neutron scattering experiments have established a penetration of RNA into the protein shell (Jacrot et al. 1976; Chauvin et al. 1978; Zulauf et al. 1981) which is pH dependent, as is the size of the capsid in the virion. Further, it was found (Cuillel et al. 1983 a) that the size of the capsids formed in the absence of RNA depends on the physical environment as well as on the history of the protein. Different capsids are formed depending on whether they are obtained by lowering the pH slowly or by pH jump.

These static structural investigations on the assembly and disassembly of the coat protein which should contribute to a better understanding of viral morphogenesis and decapsidation, have been complemented by a kinetic study. In a first series of experiments (Cuillel et al. 1983 b) it was shown that the self assembly of the protein is a fast process at least at the concentrations required for neutron scattering. Analysis of the results suggested the presence of intermediate species

* To whom offprint requests should be sent

but the precision of the data was insufficient to characterize them. These experiments were repeated using stopped flow techniques with synchrotron radiation X-ray solution scattering. Since X-ray scattering by protein solutions with concentrations below 1 mg/ml gives a very poor signal to noise ratio, light scattering was used to study the phenomena at low concentration.

We present in this paper the results of these studies. X-rays scattering spectra have been recorded at the EMBL Hamburg Outstation.

Materials and methods

a) Protein preparation

BMV was multiplied on barley and purified as described by Pfeiffer and Hirth (1974). BMV protein was prepared by dissociation of virus suspensions in 1 *M*-$CaCl_2$ at pH = 6.6 (Yamazaki and Kaesberg 1963). After centrifugation at 7,000 *g*, the supernatant, containing the dissociated protein was dialysed against a buffer (pH 7.1) with 10 m*M* sodium cacodylate, 500 m*M* KCl and 5 m*M* $MgCl_2$. The undegraded virus was eliminated by a high speed centrifugation (4 h at 280,000 *g*). Protein concentrations were determined spectrophotometrically using an extinction coefficient of 0.82 at 280 nm (Cuillel et al. 1983 a).

b) Light scattering

Time resolved light scattering measurements were performed with a fluorimeter (Dupont 1982) and designed for maximum lamp stability and efficiency of light detection using interference filters. Transient scattered light was recorded at 90° (incident wavelength 345 nm), using the stopped-flow device manufactered by Bio-Logic (Meylan, France). The dead time of this device is around 5 ms).

c) X-ray scattering

X-ray solution scattering experiments were performed on the X33 double focusing monochromator-mirror camera (Koch and Bordas 1983) on the storage ring DORIS of the Deutsches Elektronen Synchrotron (DESY) in Hamburg. The wavelength was 0.15 nm. Data were collected with a position sensitive quadrant detector (Boulin, Gabriel and Hendrix unpublished) using a (70:30) Argon/CO_2 mixture at atmospheric pressure. The data acquisition system (Boulin et al. 1982) and processing systems (Boulin et al. 1986) have been described elsewhere. For the time resolved experiments a stopped flow device based on the constant flow principle was used. Details of the design of this instrument have been given elsewhere (Berthet-Colominas et al. 1984). Briefly, gas pressure drives the reagents through the mixing chamber to a measuring cell. This cell is 1 mm thick and has two 20 μm thick mica windows with a cross-section of $8 \times 4\ mm^2$. The overall deadtime of the device resulting from the mixing time and the filling time of the measurement cell is 80 ms.

For each shot, 60 μl of a protein solution in neutral buffer (10 m*M* sodium cacodylate buffer pH = 7.1, 500 m*M* KCl and 5 m*M* $MgCl_2$) were mixed with an equal volume of acetate buffer so as to bring the pH down to 5.0. The time sequence used to record the scattering patterns depended on the concentration (the rate of the assembly is a function of the concentration). For a concentration of the protein at pH = 7 of 8 mg/ml the time sequence was

2×10 ms, 20×40 ms, 30×100 ms, 20×400 ms, $33 \times 1{,}000$ ms .

Between successive shots the mixing chamber and the cell were washed with buffer at pH 5.0. Shots were recorded in groups of about 20; each group was stored on disc and checked for possible artefacts. All valid subsets were normalised to the intensity of the primary beam as monitored by an ion chamber and to the duration of each frame. They were then added to produce a final set of averaged data.

e) Data analysis

When the concentration of a solution is sufficiently low to neglect interparticle interference the intensity scattered by a polydisperse solution containing particles of n different types can be expressed as

$$i_t(Q) = \sum N_k\, i_k(Q)\,,$$

where N_k is the number of particles k existing in the solution at time t and $i_k(q)$ is the scattering curve of a particle of type k. Q is the scattering vector related to the wavelength λ and to the scattering angle 2θ by:

$$Q = 4\pi \sin\theta/\lambda\,.$$

We assume that polymerization occurs by a incorporation of small aggregates (dimers) in a spherical shell to give ultimately an empty capsid, then each type of particle k will contain an integral number of dimers m_k and the scattering curve $i_k(Q)$ of each species k can be approximated by the scattering curve of a spherical shell with a hole of variable size. This scattering curve can be calculated as shown by Witz and Kruse (1983) for a thick hollow sphere of internal and external radii R_1 and R_2 with a hole of half-angle φ. Under these

conditions, the scattered intensity is given by:

$$i_k(Q) = \sum_{m=0}^{\infty} i_m(Q)$$

$$i_k(Q) = \sum_{m=0}^{\infty} \frac{[P_{m+1}(\cos\varphi_k) - P_{m-1}(\cos\varphi_k)]^2}{(2m+1)\,16\pi^2\,\varphi^6} \cdot \left[\int_{\varphi R_1}^{\varphi R_2} \chi^2 j_m(x)\,\mathrm{d}x\right]^2,$$

where j_m are the spherical Bessel functions and P_m the Legendre polynomials. If at $t = 0$ the solution contains N_T dimers, at any time t of the polymerization we can write:

$$i_t(0) = \sum_k N_k\, i_k(0) = N_t\, i_D(0) \sum \lambda_k m_k$$

$$R_G^2 = \frac{1}{i_t(0)} \sum_k N_k\, i_k(0)\, R_{G,k}^2$$

$$i_t(Q) = \sum_k N_k\, i_k(\varphi) = N_t \sum_k \frac{\lambda_k}{m_k}\, i_k(\varphi),$$

where $i_D(0)$ is the intensity scattered at $Q = 0$ by a dimer; m_k is the number of dimers contained in a particle of type k and λ_k/m_k, the fraction of dimers contained in the particles of type k with:

$$N_k = \lambda_k N_T/m_k \qquad \sum \lambda_k = 1\,.$$

With a least squares program which minimises χ^2, a set of $\lambda_k(t)$ can be determined.

$$\chi^2 = \frac{1}{\sigma_\varphi} \sum_A \left| \sum \frac{\lambda_k}{m_k}\, i_k(\varphi) - i_{obs} \right|^2 .$$

A is a set of points at which observations have been made and σ_q is the standard deviation.

Results and data analysis

a) X-ray scattering

Experiments were performed at two protein concentrations: 4 mg/ml and 0.8 mg/ml after mixing. For the more dilute sample the signal to noise ratio was too low for a meaningful analysis. We thus concentrate here on the 4 mg/ml data. The experiment was repeated 430 times. After inspection all the data were kept, normalised and averaged (see Materials and methods). They were subsequently corrected for detector response and background. Some of the resulting spectra are shown in Fig. 1.

Within 1 s after mixing a shoulder can be seen which turns, a second later, into a minimum which gradually deepens. This suggests that spherical particles are very quickly formed in detectable amount and represent an increasing fraction of the protein in solution.

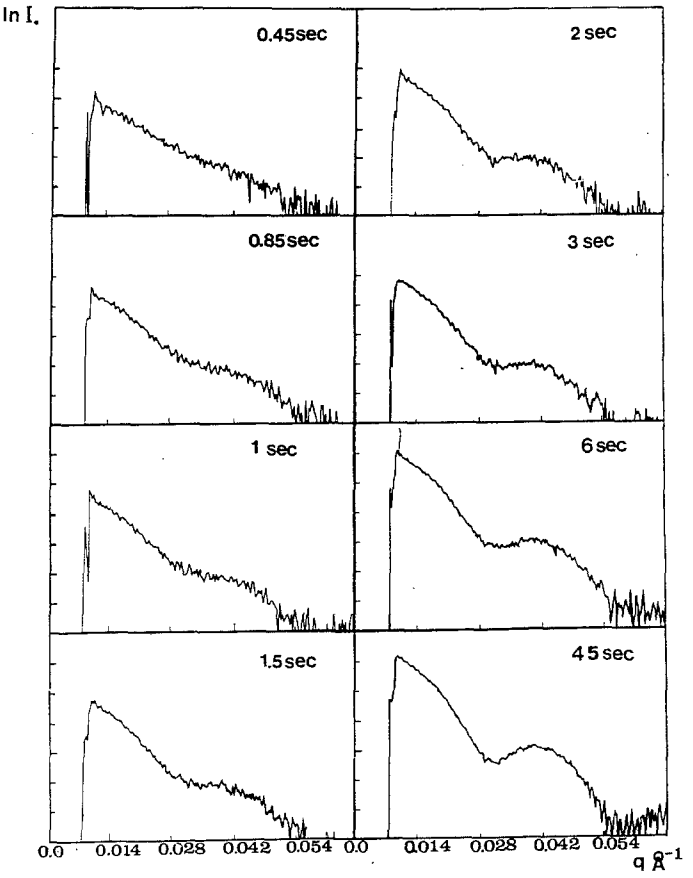

Fig. 1. Typical X-ray scattering curves collected at various times after induction of the polymerisation by a pH jump. The logarithm of the intensity is plotted as a function of $q = 4\pi^* \sin\theta/\lambda$ where 2θ is the scattering angle and λ the wavelength of the X-ray (1.4 Å)

Estimates of I_0 and R_g were derived from a Guinier analysis (Guinier and Fournet 1955). The range of Q-values used for this analysis corresponds to $1.5 < Q \cdot R_g < 2.2$ for the largest value of the radius of gyration (110 Å). This leads to some overestimate of those largest values of R_g. This does not, however, qualitatively affect the results shown in Fig. 2. The evolution of I_0 with time reflects the kinetics of the overall polymerisation. Here again, the speed of the process is apparent with, for instance, a half-time of about 6 s. More importantly, the kinetics are very complex: $I_0(t)$, far from being a single exponential displays a very fast initial phase followed by a gradual slow down; clearly, several processes occur in parallel with different time constants. The radius of gyration increases much faster than the intensity at the origin: this was to be expected, since they are different averages (see Materials and methods), which explains why the largest radii soon dominate the distribution.

We have also plotted the evolution with time of the intensity in the region of the first minimum. As can be

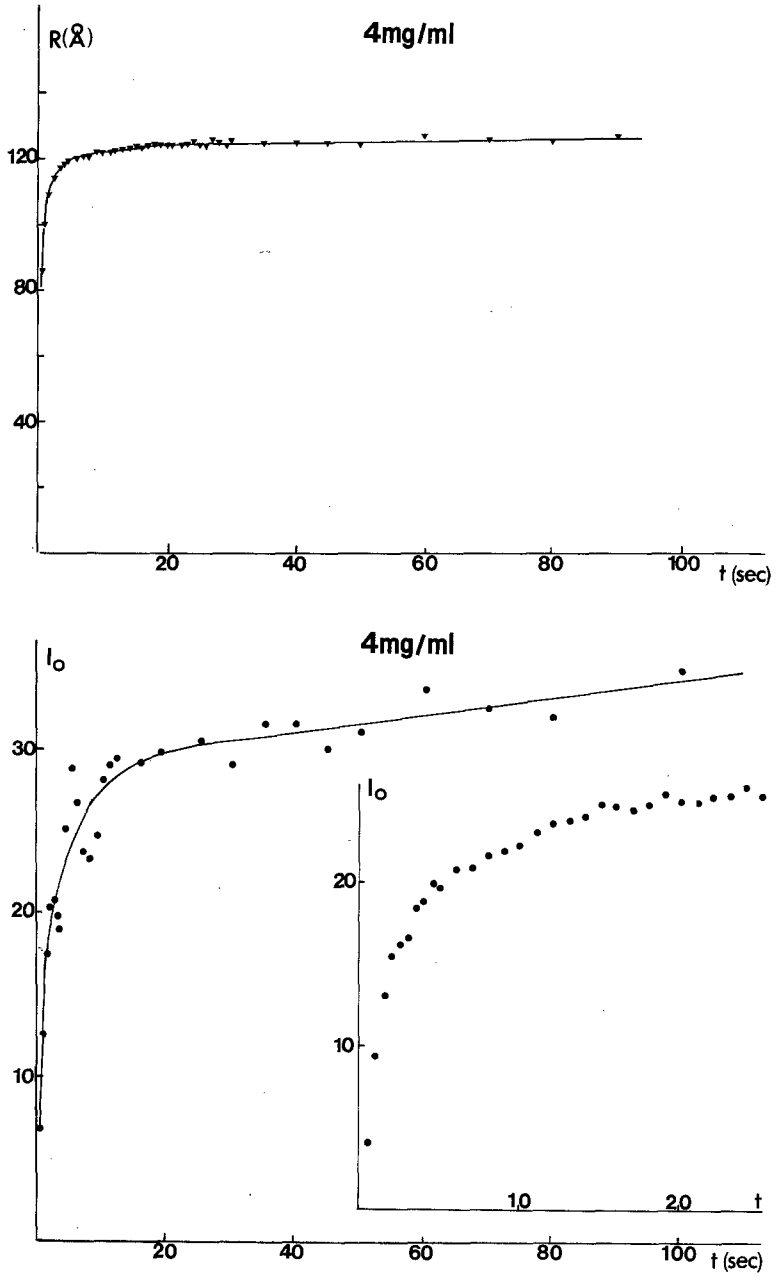

Fig. 2. Time variation of the radius of gyration and of the intensity at the origin in the X-ray scattering measured with a protein solution of 4 mg/ml. The insert gives the variation of the intensity at the origin during the first 20 s

seen in Fig. 3 a, it first increases, reaches a maximum after 1 s before decreasing as the minimum deepens. This directly proves the presence in solution of intermediate states of aggregation in significant amount (Moody et al. 1983) (see Fig. 3).

This is as much as can be directly obtained from our X-ray scattering data. Any further interpretation requires a model against which to test our data. For this, we turned to electron microscopy. A solution of coat protein was deposited on a grid a few seconds after the pH jump and negatively stained with uranyl acetate. Together with apparent full capsids, incomplete capsids could be seen with the same apparently radius but still lacking part of their shell. However, a staining artefact could not be ruled out with the stain inducing a partial dissociation, thus shifting the distribution of particles towards smaller fragments. In order to check for this possibility, we resorted to cryo-electron microscopy on frozen hydrated samples (Adrian et al. 1984). A solution of coat protein was very quickly frozen during the polymerisation. The pictures obtained (see Fig. 4) confirm the presence in solution of spherical shells at all the stages of formation, from small aggregates to capsids.

These observations suggest that the assembly proceeds by juxtaposition of small building units to form particles of increasing weight and constant curvature up to a closed spherical shell: the complete

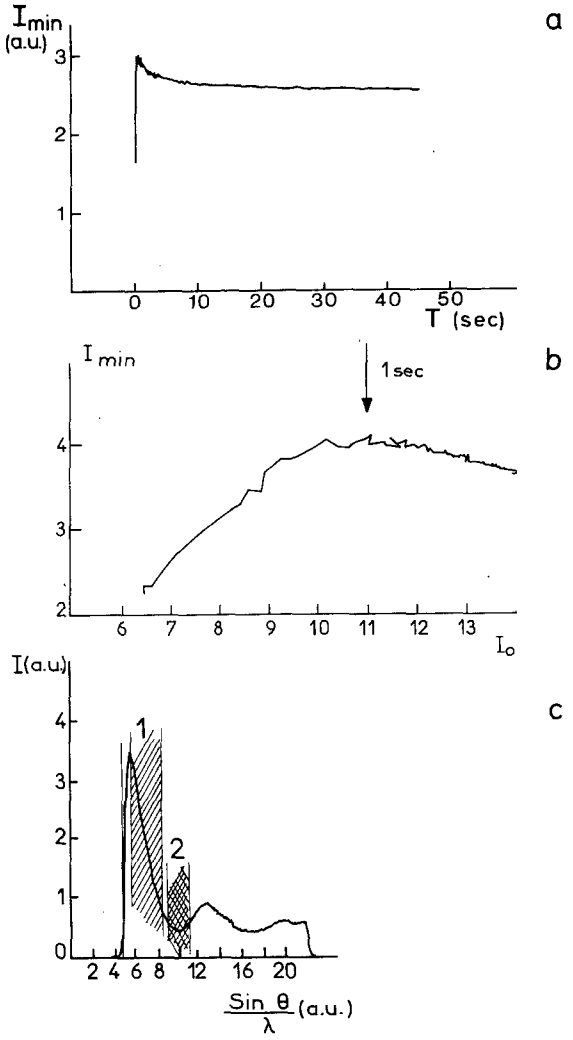

Fig. 3. **a** Evolution of the intensity in the region of the first minimum. **b** Variation of the intensity in the the vicinity of the first minimum of the scattering curve as a function of the intensity near the origin. **c** Shows the range of scattering angles over which the intensities have been added to improve the statistical accuracy. If the sample was at any time essentially a mixture of protein in their initial state (dimers) and in their final state (capsid) the derivative of these variation would have a constant sign and no maximum would be observed

capsid. At any time during the assembly, the solution would then contain spherical shells in all stages of formation. To test this model against our X-ray scattering patterns, we make several assumptions and approximations:

i) Only dimers of the coat protein are present in solution at neutral pH.
ii) The building unit is a dimer.
iii) The capsid is modeled as a single spherical shell of homogeneous density.
iv) Each fragment is modeled as a spherical shell with a single circular hole with a half-angle at the centre of the sphere φ (see Materials and methods).

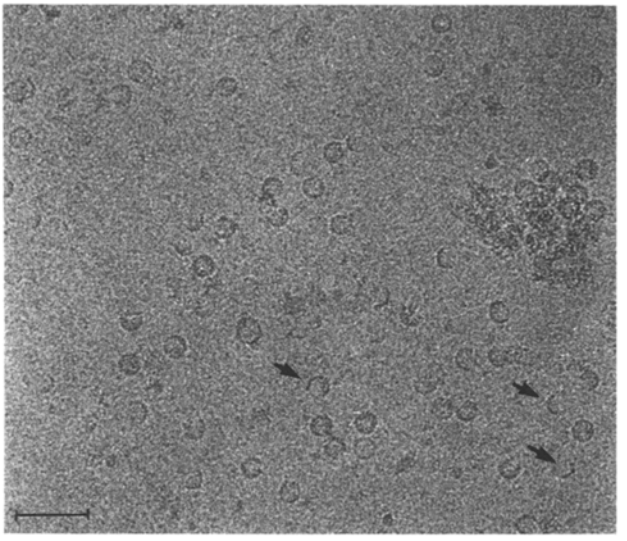

Fig. 4. Image of a protein solution of 0.2 mg/ml 300 s after pH jump. The sample is observed by cryoelectron microscopy (Adrian et al. 1984). The bar length correspond to 100 nm

v) We restrict ourselves to five classes of intermediates; each class is defined by the half-angle at the centre of the sphere. The five selected classes are:

- $\varphi = 169°$ dimer
- $\varphi = 135°$ 13 dimers
- $\varphi = 90°$ half-capsid
- $\varphi = 54°$ 71 dimers
- $\varphi = 0°$ complete capsid .

vi) We ignore size polydispersity as there was no clear indication of it from electron micrographs.

The outer and inner radii of the shell were determined using the final scattering pattern. Values of 13.4 nm and 8.0 nm for the outer and inner radii respectively were obtained, in good agreement with the values derived from the model of the virus (Chauvin et al. 1978; Zulauf et al. 1981). We then attempted to analyse the intermediate scattering patterns assuming first that only two species coexist at a given time t. We were unable to fit the experimental scattering curves with the λ_k derived from $I_0(t)$ and the condition $\sum \lambda_k = 1$ (see Materials and methods).

Three classes of particles were necessary to fit I_0 and R_g values as well as the complete scattering curves. We proceeded as follows: a first approximation of the $\lambda_k(t)$ was derived from the I_0 and R_g values together with the condition $\sum \lambda_k = 1$. Those values were then used as a starting point for a least-square fit of the whole scattering curve. The resulting set of $\lambda_k(t)$ is

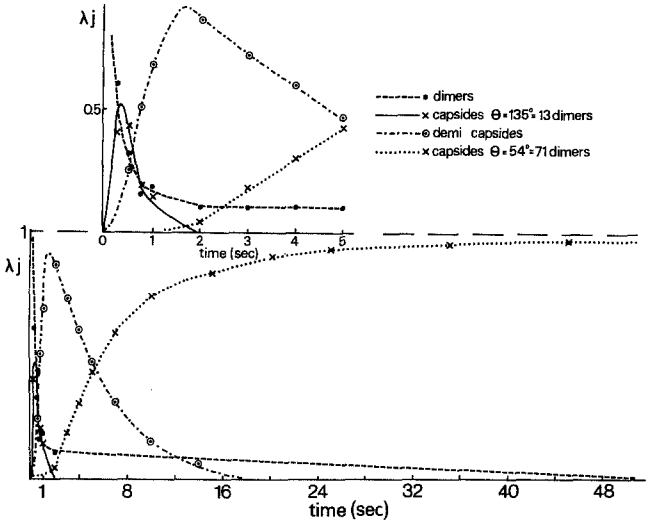

Fig. 5. Time behaviour of the four subclasses of incomplete capsids used for the analysis of the X-ray data. The behaviour during the first 5 s is given in the top part of the figure

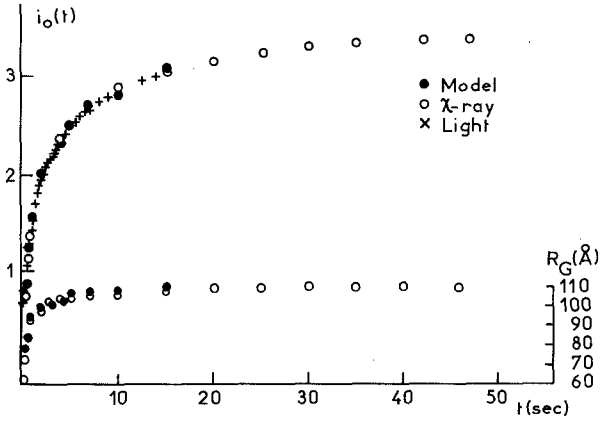

Fig. 6. Comparison between the experimental data (X-ray and light scattering) with the values derived from our model for the assembly of the capsid. The comparison is made for the radius of gyration and the intensity at the origin

plotted in Fig. 5. It should be noted that we could not include any significant amount of complete capsids even in the final spectra without having to introduce an unrealistic amount of dimers preventing us from keeping the total scattering mass constant. We thus further approximated our complete capsids by the so-called "quasi-complete capsids" which are particles with a 54° hole corresponding to 71 dimers. This reduces the total number of species down to 4.

Estimates of $I_0(t)$ and $R_g(t)$ were derived from the same set of λ_k. Calculated and observed values are plotted in Fig. 6 and show a good agreement. Some X-ray curves are plotted in Fig. 7 together with the computer fit. They agree reasonably well, especially if one keeps in mind the small number of particles included in the computation.

b) Light scattering

As mentioned earlier, experiments were performed at 0.8 mg/ml. Although they showed very poor statistics, the time course of assembly seemed to be much slower than that observed at 4 mg/ml. This prompted us to undertake a systematic study of the concentration dependence of assembly. Light scattering was chosen because of the large signal associated with the capsid formation, even at low protein concentration. The intensity of scattered light is directly comparable to the X-ray intensity at the origin.

The evolution of the scattered light intensity is shown in Fig. 8 after correction for solvent scattering and background and division by protein concentration. The concentration dependence of scattered intensity at the time $t = 0$ (neutral pH, before mixing) is stronger than expected for a monomer-dimer equilibrium; this confirms the presence of oligomers whose number and possibly size increase with the concentration as already suggested by previous experiment (Cuillel et al. 1983 a).

We have compared the intensity of light and the X-ray intensity at the origin scattered by a solution at a protein concentration of 4 mg/ml. The light scattering data have been scaled to the X-ray value 15 s after the pH jump and superimposed on the I_0 plot of Fig. 6. The agreement between the two data sets is excellent.

The intensity of light scatterd by a solution at a protein concentration of 1.4 mg/ml was analysed in the same way as X-ray data. The results are plotted in Fig. 9. The general pattern is similar to that obtained at 4 mg/ml with X-rays, indicating that the assembly pathway is the same at these two concentrations, but the time scale is very different. The number of half-capsids, for instance, is maximal after about 17 s as compared to 2 s at 4 mg/ml. Altogether, the polymerisation is about 10 times slower. The kinetics of the assembly show a strong dependence on protein concentration. We should mention that this property was of importance in the preparation of the grids for cryo-electron microscopy. The solution of coat protein was frozen 300 s after the pH jump which triggered the polymerisation. The concentration of the solution was as low as 0.2 mg/ml. Because of the very strong concentration dependence of the speed of polymerisation, the process was thus far from being over, even after 300 s, and no fast mixing was required.

In order to summarise all the kinetic information from light and X-ray scattering as well and to compare them in an easy way, we looked for a linear, dimen-

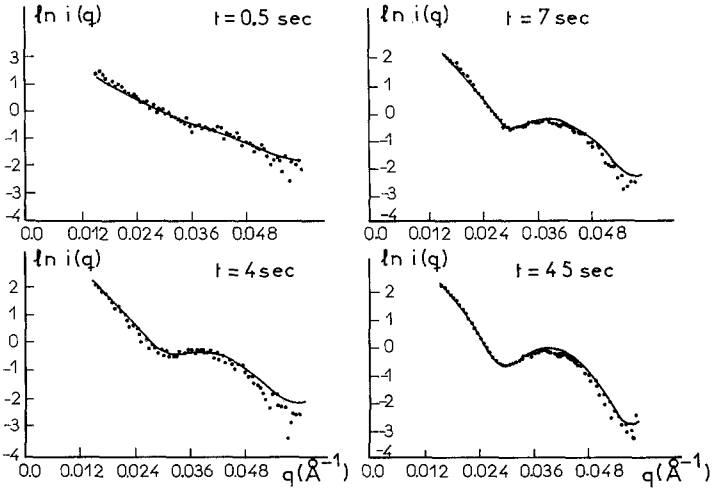

Fig. 7. Comparison between the experimental data (X-ray scattering curves) with those derived from our model. The comparison is done here on the scattering curve $I(q)$ at various time

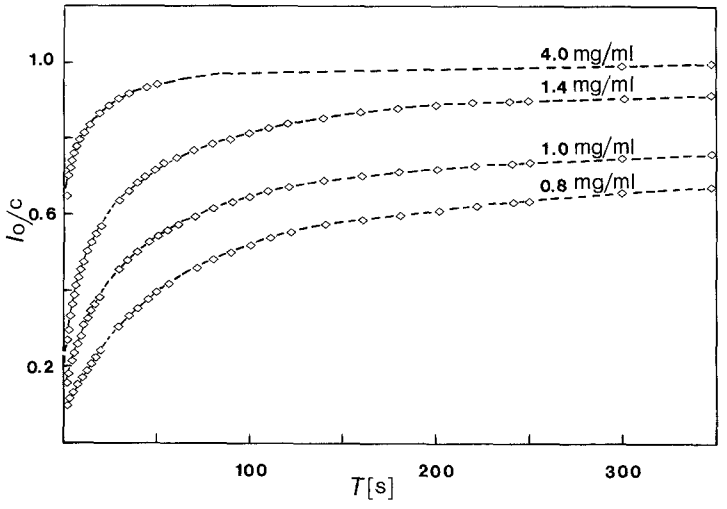

Fig. 8. Time dependance of the intensities of scattered light at 90° for different protein concentrations. At the higher concentration the intensity of X-rays scattered at the origin is plotted after normalisation of the values at 10 s. The intensities are in arbitrary units but can be compared at the various concentrations

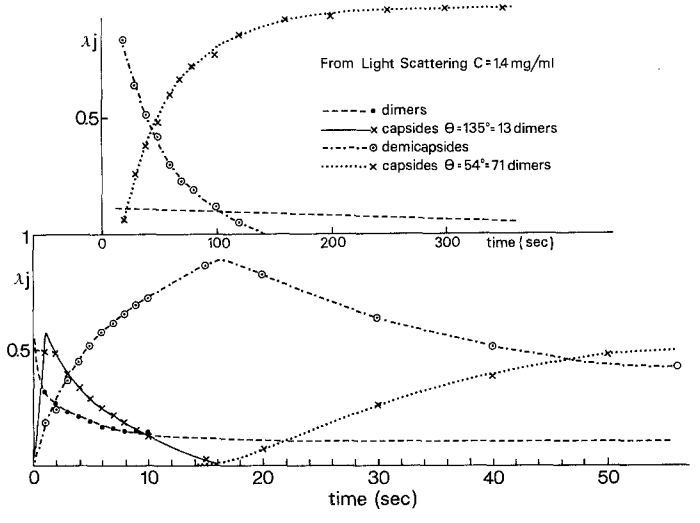

Fig. 9. Analysis of light scattering with the model used for the analysis of X-ray data (see text)

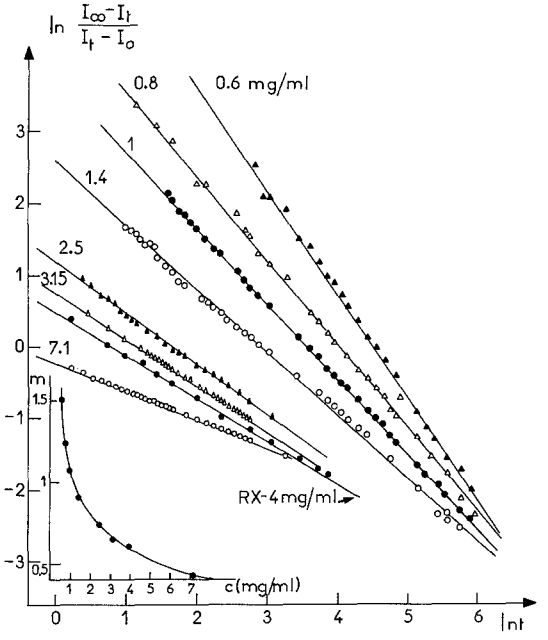

Fig. 10. Double logarithmic plot of $I_\infty - I_t/I_t - I_0$ versus time. With that representation all the data can be put together. A linear variation is observed over a large time scale. The insert show the concentration dependance of the slopes

Table 1. Fraction of final polymerisation $(I(t)/I_\infty)$ as a function of time and initial concentration

Time C	1 s	10 s	100 s
0.5 mg/ml	0.0006	0.024	0.495
1	0.014	0.16	0.72
1.5	0.054	0.32	0.80
2	0.115	0.45	0.84
5	0.48	0.75	0.90
10	0.71	0.85	0.93

sionless empirical representation. As shown in Fig. 10, a linear representation was obtained using the expression:

$$I_t = I_{t=0} + [I_{t=\infty} - I_{t=0}]\frac{1}{1 + A\,t^{-m}}$$

with

$$m \quad = 1.13\,c^{-1/2}$$

$$\log A = 7.55\,c^{-1/2} - 3.3\,.$$

This expression gives an excellent analytical approximation of the data over a large concentration range (0.6 mg/ml, 7 mg/ml) and a time scale from 1 s up to 400 s. The percentage of global polymerisation reached at any given time and concentration can be easily derived from the above expression (see Table 1). The strong concentration dependence of the rate of polymerisation is best visualised by the variation with concentration of the slope of the straight line as shown on the inset of Fig. 10. This slope varies like the inverse of the square root of the concentration.

Discussion

We were interested in both the structural and the kinetic aspect of BMV capsid assembly. As regards the structure, electron micrographs suggested a plausible model for assembly. Its validity was tested against our X-ray data. Some of the approximations involved in the computations deserve some comments.

We first assumed that only dimers of the coat protein are present in the solution at neutral pH. This seems to be a rather crude approximation, since we know from light and neutron scattering experiments that, in these conditions, there is a dynamic equilibrium between monomers, dimers and small oligomers (Cuillel et al. 1983 a). However, dimers are by far the most numerous species, even at the concentration used for X-ray scattering.

Secondly, the building unit is a dimer. This is actually a two-fold restriction: there is a unique building unit and it is a dimer. In the absence of any contradicting evidence, unicity was introduced for reasons of simplicity. As for the nature of the building block, the dimer is the first, most obvious choice in the absence of extraneous information. X-ray data were also analysed using a hexamer as a building unit. In this hypothesis, the variation with time of the concentration of each species $\lambda_k(t)$ is qualitatively the same, only the absolute value of the percentage changes. The difficulty in determining the building unit is due to the fact that the solutions are polydisperse and therefore the scattering curves cannot be used for unambigous characterisation of one of the components which is, in addition, that having the smallest molecular weight. Thus the nature of the building block cannot be determined from our X-ray scattering spectra.

The capsid is modelled as a single spherical shell of uniform density. In fact, it is known from neutron scattering studies of the virus (Chauvin et al. 1978; Zulauf et al. 1981) that the protein in the nucleocapsid is not located in a unique spherical shell with an homogeneous density distribution, but in three different shells of which the inner one is mixture of RNA and protein. Nevertheless, neutron scattering data from capsids are analysed in term of an unique shell (Cuillel et al. 1983 a). In any case, the possible disorder of the internal part of the capsid would give rise to density changes of limited amplitudes and affect only a minor fraction of the scattering mass.

Fragments are described as spherical shells with a single circular hole. This is an oversimplification considering the variety of intermediate species of any

given number of dimers which are likely to be formed, but it is in keeping with the other approximations involved, particularly the limited number of classes taken into account. This is done to minimize the number of parameters to be refined in agreement with E.M. observations.

The limits of our simplified model are most apparent in our failure to include a significant amount of complete capsids to fit even the final spectra. The instrumental parameters such as the finite size of the beam, the wavelength dispersion and the beam convergence which are convoluted with the scattering curves cannot explain this filling in of the minima: their contributions are negligible in the apparatus used. The analysis of our data in terms of a few species of which only 3 are present at the same time, can be the cause of this effect. The use of an analytical approach to determine the starting point in the last squares prevents the multiplication of the number of parameters that can be considered. Alternatively, this could be caused by size polydispersity of the spherical shell which would significantly smear the minimum and allow our data to be fitted using complete capsids. Although the occasional capsid can be seen with an apparent smaller radius on electron micrographs, there is no indication of a significant polydispersity. We thus prefer to use the "quasi-complete capsids" approximation rather than to introduce a new factor which could only be used in an ad hoc way. On the whole, the model presented here gives a crude but not unrealistic description of the assembly process.

Another possible mechanism for reconstitution could be via a scaffold constituted by the elements having the strongest interactions which is filled-in progressively by the elements having weeker interactions. In this hypothesis, however, there would be an instant in the polymerisation, when the solution consists predominantly of scaffolds giving a scattering curve with deeper minima corresponding to such a symmetrical particle. This effect does not occur in our observed data.

As for the kinetics of the process, most information has been obtained from light scattering measurements. The two main features of the kinetics are its complexity and its strong concentration dependence.

We have tried to approach the problem of virus assembly by the analysis of the kinetics behaviour of the self assembly of an empty capsid. In the system chosen it is known from previous work that the protein forms empty capsids at low pH, whereas at basic pH the protein is only present in the form of low molecular weight aggregates. It is also known that a pH jump will induce the polymerisation of those aggregates into an empty capsid of similar size to the viral capsid but of lower molecular weight whereas a slow change in pH leads to the formation of empty capsids larger than viral capsids. This has been interpreted by the existence of two conformational states of the protein separated by a barrier of potential. At basic pH the conformation is such that protein protein assembly would lead to a "sphere" of the same radius as that of the virus. When the pH is brought to a value such that the reduction of electric repulsion make this assembly possible, with a pH jump the protein keeps its high pH form and a capsid of the appropriate size is obtained. On the other hand if one approaches low pH slowly, then the protein has the time to reach its low pH form which is unable to give rise to a capsid of the right diameter. This view is borne out by potentiometric titration on CCMV (Jacrot 1975) and BMV (Pfeiffer and Durham 1977) proteins which reveals the existence of an hysteresis loop around pH 6 which proves the existence of two states of the protein. A method of in vitro virus assembly has been derived from this observation which suggests that the high pH conformation of the protein is appropriate for viral assembly. Thus, the experiments that we are reporting here on the kinetics of capsid assembly induced by pH jump are likely to be relevant for the understanding of virus assembly.

We already knew from our previous work that this capsid formation was a very fast process proceeding through intermediate states. In the work described in this article we have attempted to indentify those states. We find that the data could very well be explained by a progressive building of the capsid obtained by the addition of bricks. We can follow the time behaviour of several classes of incomplete capsids; but we have been unable to identify unambiguously the nature of the building units which could be dimers or preassembled oligomers. The kinetics are found to be very strongly concentration dependent. Combining X-ray and light scattering, data have been collecting over a concentration range of a decade which correspond to a change of time scale by two orders of magnitude. From the values in Table 1, it appears that the time required for a given fraction of polymerisation varies approximately on the inverse of the square of the concentration, i.e. on the probability of collision between molecules. This suggests that the rate of capsid assembly is limited by this probability of collision. The virus assembly is a more complex reaction as it involves the RNA encapsidation. All evidence, including the kinetic studies reported in a companion article (Cuillel et al. 1987), indicate that both in vitro and in vivo the virus morphogenesis takes place by cocondensation of protein and RNA. Then the probability of collision will also be the rate limiting factor. This could explain one of the paradoxes in viral infection, namely that the disassembly and the reassembly of the particles take place in rather similar cellular environments: when the cell is infected the virus concentration inside the cell is ex-

tremely small whereas the concentration of viral components is very large when the assembly takes place. Our data suggest that this may well be enough to shift the equilibrium in one case toward viral component and in the other case toward complete virion.

Acknowledgements. The cryo-electron microscopy pictures were taken by Jean Lepault (EMBL Heidelberg). Yves Dupont has put to our disposal his instrument of stopped-flow for light scattering and has advised us on the way of using it. Stephan Cusack has helped us in transferring data to our computer and in writing programs. He and Peter Timmins are also be acknowledged for useful discussions.

References

Adrian M, Dubochet J, Lepault J, McDowall AW (1984) Cryo-electron microscopy of virus. Nature 308:32–36

Berthet-Colominas C, Bois JM, Cuillel M, Sedita J, Vachette P (1984) An apparatus for stopped-flow X-ray scattering. Rev Phys Appl 19:769–772

Boulin C, Dainton D, Dorrington E, Elsner G, Gabriel A, Bordas J, Koch MHJ (1982) Systems for time resolved measurements using one-dimensional and two-dimensional detectors requirements and practical experience. Nucl Instrum Methods 201:209–220

Boulin C, Kempf R, Koch MHJ, McLaughlin (1986) Data appraisal evaluation and display for synchrotron radiation instruments: hardware and software. Nucl Instrum Methods A249:399–407

Chauvin C, Pfeiffer P, Witz J, Jacrot B (1978) Structural polymorphism of bromegrass mosaic virus: a neutron small angle scattering investigation. Virology 88:138–148

Cuillel M, Zulauf M, Jacrot B (1983a) Self assembly of brome mosaic virus protein into capsids: initial and final states of aggregation. J Mol Biol 164:589–603

Cuillel M, Berthet-Colominas C, Krop B, Tardieu A, Vachette P, Jacrot B (1983b) Self assembly of brome mosaic virus capsids: kinetic study using neutron and X-ray solution scattering. J Mol Biol 164:645–650

Cuillel M, Berthet-Colominas C, Timmins PA, Zulauf M (1987) Reassembly of brome mosaic virus from dissociated virus. Eur Biophys J 15:161–168

Dupont Y (1982) Low temperature studies of the sarcoplasmic reticulum calcium pump. Biochim Biophys Acta 688:75–87

Guinier A, Fournet G (1955) Small angle scattering of X-rays. John Wiley, New York

Jacrot B (1975) Studies on the assembly of a spherical plant virus. J Mol Biol 95:433–446

Jacrot B, Pfeiffer P, Witz J (1976) The structure of a spherical plant virus (brome mosaic virus) established by neutron diffraction. Philos Trans R Soc London Ser B 276:109–112

Kaper JM (1975) The chemical basis of virus structure, dissociation and reassembly. North-Holland, Amsterdam

Koch MHJ, Bordas J (1983) X-ray diffraction and scattering on disordered systems using synchrotron radiation. Nucl Instrum Methods 208:461–469

Moody MF, Vachette P, Foote AM, Tardieu AM, Koch MHJ, Bordas J (1983) Stopped-flow X-ray solution scattering: the dissociation of aspartate transcarbomylase. Proc Natl Acad Sci USA 77:4040–4043

Pfeiffer P, Hirth L (1974) Aggregation states of brome mosaic virus protein. Virology 61:160–167

Pfeiffer P, Durham ACH (1977) The cation binding associated with structural transitions in bromegrass mosaic virus. Virology 81:419–432

Steven AC, Smith PR, Horne RW (1978) Capsid fine structure of cowpea chlorotic mottle virus: from a computer analysis of negatively stained virus array. J Ultrastruct Res 64:63–73

Yamazaki H, Kaesberg P (1963) Degradation of bromegrass mosaic virus with calcium chloride and isolation of its protein and nucleic acid. J Mol Biol 7:760–762

Witz J, Krusse J (1983) Small-angle scattering of open isomeric capsids. Eur J Biochem 137:47–55

Zulauf M, Cuillel M, Jacrot B (1981) Neutron and light scattering studies of brome mosaic virus and its protein. In: Chen SH, Chu B, Nossal R (eds) Scattering techniques applied to supramolecular and nonequilibrium systems. Plenum Press, New York